This is a preprint, the final version is subject to change, of the American Mineralogist (MSA)
Cite as Authors (Year) Title. American Mineralogist, in press.
(DOI will not work until issue is live.) DOI: http://dx.doi.org/10.2138/am-2017-5720

Revision 1

Adakite metasomatism in a back-arc mantle peridotite xenolith from the Japan Sea

Yuji ICHIYAMA[1], Tomoaki MORISHITA[2], Akihiro TAMURA[2] and Shoji ARAI[2]

1: Earth Science Department, Chiba University, Yayoi 1-33, Inage, Chiba 263-8522, Japan

2: School of Naturel System, Kanazawa University, Kakuma, Kanazawa 920-1192, Japan

Abstract

Secondary orthopyroxenes occur as veinlets (<0.1 mm thick) cutting an olivine in a two-pyroxene peridotite xenolith from the Shiribeshi Seamount in the Japan Sea. These orthopyroxenes are characterized by low Al_2O_3 (0.4–1.7 wt%), Cr_2O_3 (<0.1 wt%), and CaO (0.3–0.4 wt%) contents, which are the same signatures of the secondary orthopyroxenes in peridotite xenoliths from island arcs. The trace-element patterns of the melts in equilibrium with the secondary orthopyroxenes show enrichment in light rare earth element and Sr and depletion in heavy rare earth element, Nb and Ti. These trace-element characteristics are highly consistent with those of slab-derived adakites. The involvement of slab-derived melts in the mantle beneath the Japan Sea has been inferred from the geochemical characteristics of the volcanic rocks formed during opening of the Japan Sea. The source mantle of the enriched basalts in the Japan Sea is likely to have been metasomatized by adakitic melts in the same manner as the peridotite-hosted veinlet. The secondary orthopyroxenes in the peridotite xenolith from the Shiribeshi Seamount provide direct evidence for the metasomatic influx of adakitic melts into the back-arc mantle beneath the Japan Sea. Adakitic metasomatism, as documented in the Japan Sea, potentially plays an important role in mantle evolution and magma generation beneath global back-arc basins.

Key-words: Mantle xenolith, Secondary orthopyroxene, Japan Sea, Adakite

INTRODUCTION

The addition of H_2O drastically reduces the solidus temperatures of mantle peridotites (Kushiro, 1972); therefore, the influx of H_2O-rich substances released from the subducting slab into the overlying mantle wedge contributes significantly to the genesis of island arc magmatism (e.g., Tatsumi and Eggins, 1995). Recent active petrological investigations of peridotite xenoliths from island-arc volcanoes have

provided possible evidence for metasomatism caused by inputs of subduction components released from the subducting slab. In particular, secondary orthopyroxene replacing olivine appears in island-arc peridotite xenoliths (e.g., Arai and Kida, 2000; Arai and Ishimaru, 2008; Bali et al., 2007; Bénard and Ionov, 2012, 2013; Franz et al., 2002; Grégoire et al., 2001; Halama et al., 2009; Ishimaru et al., 2007; McInnes et al., 2001, Shimizu et al., 2004). The presence of such secondary orthopyroxene implies that a possible metasomatic reaction between slab-derived Si-rich melts or fluids and peridotites in the mantle wedge takes place beneath island arcs. Ishimaru et al. (2007) and Shimizu et al. (2004) proposed that orthopyroxene replacing olivine between peridotite and felsic rock vein in island-arc peridotite xenoliths resulted from the reaction with slab-derived adakitic melts. Moreover, metasomatic melt inclusions with adakitic geochemical affinities have been also reported in island-arc peridotite xenoliths (Bali, 2008; Schiano et al., 1995).

Several overviews of global back-arc magmatism and mantle processes from the viewpoint of petrology and geochemistry of back-arc basin basalts (BABB) have been carried out (e.g., Pearce and Stern, 2006; Taylor and Martinez, 2003), but studies using mantle peridotites have not yet been performed, due to their rarity. The Japan Sea is a Miocene back-arc basin formed by the detachment of the Japan arcs from the Asian continent (e.g., Kaneoka et al., 1992; Nohda, 2009; Otofuji et al., 1985; Tamaki et al., 1992). We have recently discovered mantle peridotite xenoliths enclosed in basaltic to andesitic lavas from the Shiribeshi Seamount in the Japan Sea (Ichiyama et al., 2013, 2016; Fig. 1). Interestingly, veinlet-like secondary orthopyroxenes replacing olivine, as observed in island-arc peridotite xenoliths, are present in a sample of these peridotite xenoliths. The secondary orthopyroxenes in the peridotite xenolith from the Japan Sea can provide important information on the mantle metasomatic processes during the Japan Sea opening, and possibly global back-arc basins worldwide. In this study, we present new geochemical data for the secondary orthopyroxenes in the mantle peridotite from the Japan Sea, and discuss their petrogenesis and significance for Japan Sea magmatism.

BRIEF OVERVIEW OF THE JAPAN SEA AND DESCRIPTION OF THE PERIDOTITE XENOLITHS FROM THE SHIRIBESHI SEAMOUNT

The Japan Sea has three main topographic basins: the Japan Basin, the Yamato Basin, and the Tsushima Basin (Fig. 1). The basement of the Japan Basin is composed of basaltic oceanic crust formed during Miocene back-arc spreading, whereas those of the Yamato Basin and Tsushima Basin are continental crust thinned or extended by

back-arc rifting (Tamaki et al., 1992). Drill sampling performed during the Ocean Drilling Program (ODP) Legs 127 and 128 obtained samples of basaltic lavas and sills interbedded with Miocene sediments from three sites in the Japan Basin and Yamato Basin (e.g., Allan and Gorton, 1992; Fig. 1). These volcanic rocks yield 17–20 Ma Ar–Ar radiometric ages, indicating formation during the Miocene opening of the Japan Sea (Kaneoka et al., 1992).

The Shiribeshi Seamount is a Quaternary submarine stratovolcano formed on the northeastern margin of the Japan Basin (Fig. 1). The Shiribeshi Seamount is a volcano on back-arc side in the Northeast Japan Arc, and is composed mainly of high-K calc-alkaline basaltic to andesitic lavas (Ichiyama et al., 2013; Shuto et al., 1991). Lava samples were collected from dive sites on the flank and around the summit of the seamount using the manned submersible *SHINKAI 2000* during cruises performed by the Japan Agency for Marine-Earth Science and Technology (JAMSTEC). The detailed metadata (collecting date, collecting point, ship name, etc.) and petrology of the host volcanic rocks with the peridotite xenoliths were provided in the GANSEKI database[1] (Ichiyama et al., 2011) and Ichiyama et al. (2013), respectively. The basaltic to andesitic lavas contain abundant small-sized peridotite xenoliths (<2 cm) of two-pyroxene peridotites (lherzolites to harzburgite) and dunites. Ichiyama et al. (2016) suggested that the two-pyroxene peridotites represent residues after decompression melting during the opening of the Japan Sea, and that the dunites are products formed via the reaction between the two-pyroxene peridotites and the pyroxene-undersaturated magmas formed prior to the host magmas. The secondary orthopyroxenes occur as thin mono-mineralogic veinlets (<0.2 mm thick) replacing olivine in a two-pyroxene peridotite (Fig. 2). Importantly, all peridotite xenoliths from the Shiribeshi Seamount have the fine-grained secondary reaction products of olivine + chromian spinel + glass formed along the boundaries between the peridotites and their host lavas, but reaction rims of orthopyroxene are not observed along any boundary.

ANALYTICAL METHODS

The major-element concentrations of the secondary orthopyroxenes and olivines in the veinlet-intruded peridotite were measured using electron microprobe analyzers installed at Chiba University (JEOL JXA-8230) and JAMSTEC (JEOL JXA-8800). Natural and synthetic minerals were used as standard samples. Acceleration voltage and beam current in the analysis were set at 15 kV and 20 nA, respectively, with a probe diameter of 3 μm. Trace-element concentrations (rare earth element [REE], Ti, Sr, Y, Zr,

[1] URL: http://www.godac.jamstec.go.jp/ganseki/search/e

Nb, and Ba) were determined using a laser-ablasion inductively coupled plasma mass spectrometer (Agilent 7500s with 193 nm ArF excimer MicroLas GeoLas Q-plus laser) at Kanazawa University with a laser spot of 110 μm. Details of the methods followed, including analytical accuracy and precision, are described in Morishita et al. (2005). Representative results are given in Table 1 for major element and Table 2 for trace element.

RESULTS

The secondary orthopyroxenes are characterized by much lower CaO (0.3–0.4 wt%), Al_2O_3 (0.4–1.7 wt%), and Cr_2O_3 (mostly <0.1 wt%) contents than those in the two-pyroxene peridotites (Fig. 3). The Mg# (= Mg/[Mg + Fe]) values are between 0.88 and 0.89. The trace-element contents of the secondary orthopyroxenes are markedly low, especially for middle REE (MREE) such as Eu, Gd, and Tb, which were below the detection limit (Fig. 4a). The primitive mantle-normalized trace element patterns of the secondary orthopyroxenes exhibit slight enrichment in light REE (LREE) without any significant troughs and spikes. The secondary orthopyroxenes differ from those in the two-pyroxene peridotites in possessing a higher LREE content (Fig. 4a).

Olivines in the veinlet-intruded two-pyroxene peridotite have values of NiO = 0.36–0.39 wt.% and MnO = 0.25–0.32 wt.% in Mg# = 0.87, and are lower in Mg# than those in the other two-pyroxene peridotites at the same NiO content (Fig. 5).

DISCUSSION

Origin of the secondary orthopyroxenes: Evidence for reaction with adakitic melts

The lack of orthopyroxene reaction rims along the boundaries between the peridotite xenoliths and the host lavas from the Shiribeshi Seamount indicates that the secondary orthopyroxenes in the peridotite xenolith cannot be attributed to the reaction with the host magmas during transportation to the surface. The secondary orthopyroxenes are characterized by lower contents of CaO, Al_2O_3, and Cr_2O_3 than those in the residual two-pyroxene peridotites and host lavas (Fig. 3). The trace-element patterns of the secondary orthopyroxenes show slight LREE enrichment, which is different from the highly depleted patterns expected for residual peridotites after simple decompression melting caused by the back-arc spreading that formed the Japan Basin (Ichiyama et al., 2016; Fig. 4a).

The reaction of olivine with Si-rich melt can generate orthopyroxene products (e.g., Kelemen et al., 1998). The petrological and geochemical evidence described above suggests that the secondary orthopyroxenes can be explained by the reaction between

the mantle peridotites and SiO_2-saturated melts. Arai and Ishimaru (2008) reviewed island-arc peridotite xenoliths and suggested that secondary orthopyroxenes in island-arc peridotites can be formed by the reaction of olivines with Si-rich liquids derived from the subducted slab. Moreover, secondary orthopyroxenes replacing olivines are generally lower in CaO, Al_2O_3, and Cr_2O_3 contents than primary residual orthopyroxene. For instance, the secondary orthopyroxenes in peridotite xenoliths from the Avacha Volcano in Kamchatka (Ishimaru et al., 2007) and from the Tallante area, Spain (Shimizu et al., 2004), are very similar to those from the Shiribeshi Seamount (Fig. 3).

The vein-like secondary orthopyroxenes in the Avacha peridotite xenoliths show a trace-element pattern similar to those in the Shiribeshi peridotite, with the exception of significant positive Zr and Hf anomalies in the former (Fig. 4a). Ishimaru et al. (2007) interpreted that the secondary orthopyroxenes in the Avacha peridotites were produced by the infiltration of slab-derived adakitic melts into the mantle wedge. In contrast, Bénard and Ionov (2013) argued that these secondary orthopyroxenes resulted from the fractionation-reactive percolation of boninite melts into the mantle wedge, which could cause the percolating melts to become enriched in LREE and Zr–Hf via assimilation and re-equilibration with peridotite wall rocks. Although the origin of the secondary orthopyroxene veins in the Avacha peridotite xenoliths is still controversial, there is no such Zr anomaly in the trace-element patterns of the secondary orthopyroxenes in the Shiribeshi peridotite; therefore, it is unlikely that fractionation-reactive percolation took place effectively in the orthopyroxene veinlets. The patterns of these veinlets are closer to those of an orthopyroxene phenocryst in a magnesian adakite from the Izu–Bonin–Mariana (IBM) arc (Li et al., 2013) than those in a typical calc-alkali island-arc andesite in the Northeast Japan arc (Kobayashi and Nakamura, 2001; Fig. 4a). We calculated the trace-element compositions of the melts in equilibrium with the secondary orthopyroxenes using two datasets of partition coefficients between orthopyroxene and melt: (1) hydrous basaltic melt and orthopyroxene experimentally determined by McDade et al. (2003); and (2) whole-rock and orthopyroxene phenocryst calculated from an IBM magnesian adakite of Li et al. (2013; Table 2). The melt compositions calculated using these two datasets are characterized by enrichment in LREE and depletion in Nb and heavy REE (Fig. 4b). Additionally, the patterns calculated using the latter partition coefficients show distinct Sr spikes and possible Ti troughs. These chemical characteristics of the calculated melt compositions are in good agreement with those of an average adakite and adakites from the IBM arc and Japan Sea (Fig. 4b). Therefore, these results suggest that the causal agent for the secondary

orthopyroxenes in the Shiribeshi Seamount was adakitic melts, which are likely generated by melting of the subducting slab (e.g., Drummond et al., 1996; Martin et al., 2005).

IMPLICATIONS FOR ADAKITIC MELT METASOMATISM BENEATH THE JAPAN SEA

Basalts drilled from the floor of the Japan Sea can be subdivided into two types on the basis of their geochemical characteristics: depleted (D-type) and enriched (E-type) basalts. D-type basalts have geochemical signatures similar to those of mid-ocean ridge basalt, whereas E-type basalts are characterized by the enrichment of large-ion lithophile elements and LREE and by radiogenic Pb isotopic composition compared with the D-type basalts (Allan and Goton, 1992; Cousens et al., 1994; Hirahara et al., 2015). Hirahara et al. (2015) suggested that the source mantle of the E-type basalts was metasomatized by the influx of melts derived from subducting slab sediments, while that of the D-type basalts was more depleted and higher mantle potential temperature than that of the E-type basalts. Tamura (2003) estimated the primary magma compositions for the D-type and E-type basalts (Fig. 5), and revealed that the E-type primary magma (and source mantle in equilibrium with it) was Fe-rich in composition relative to the D-type. Tamura (2003) proposed that slab-melt from subducted sediment possibly added to Fe-rich E-type mantle source. The presence of such slab melts is supported by the formation of Miocene adakites in back-arc margins during the opening of the Japan Sea: these adakites were derived from the melting of altered basaltic crust and sediment caused by the upwelling of the asthenospheric mantle into the mantle wedge (Fig. 4b; Sato et al., 2012). Ichiyama et al. (2016) proposed that the peridotite xenoliths from the Japan Sea were the residues after the extraction of the D-type and E-type basaltic melts, on the basis of the clinopyroxene REE and chromian spinel compositions, and that the E-type residues underwent higher degrees of partial melting than the D-type, due to the reduction of the solidus temperature possibly by H_2O supply via infiltration of the slab-derived melts.

As discussed above, the veinlet-forming secondary orthopyroxenes in the two-pyroxene peridotite xenolith from the Shiribeshi Seamount should have been produced by the infiltration of slab-derived adakitic melts. The olivines in the veinlet-intruded peridotite xenolith are plotted in a FeO-rich direction relative to those in other common two-pyroxene peridotites, while maintaining the same NiO content (Fig. 5). This should have been caused by Si-rich adakitic metasomatism because high compatibility of Ni for olivine can maintain the Ni budget for olivine during olivine consumption (Kelemen et al., 1998) despite the increase in Fe/Mg ratios. Interestingly,

the olivine composition in the veinlet-intruded peridotite is highly consistent with the calculated olivine composition in equilibrium with the primary E-type magmas estimated by Tamura (2003; Fig. 5). Metasomatism caused by adakitic melt infiltration into the mantle beneath the Japan Sea can also account for the Fe-enrichment and trace-element characteristics of the E-type basalts (Fig. 6). The secondary orthopyroxenes probably provide direct evidence for the metasomatic influx of slab-derived melts into the mantle beneath a back-arc basin in the Japan Sea. Pearce and Stern (2006) proposed, considering BABB geochemistry, that slab-derived melts (or supercritical fluid) were input into the source mantle of global BABB as a deep subduction component. Although adakitic volcanism on back-arcs is rare, adakitic metasomatism, as proposed in this study, potentially plays an important role in mantle metasomatism and magma generation beneath global back-arc basins.

1. Conclusions

(1) Secondary orthopyroxenes occur as veinlets replacing olivine in two-pyroxene peridotite from the Shiribeshi Seamount in the Japan Sea. The orthopyroxenes are characterized by low Al_2O_3, Cr_2O_3, and CaO contents, and the trace-element patterns of the melt in equilibrium with them are very similar to those of adakites. The veinlet-forming secondary orthopyroxenes in the peridotite were produced by the reaction between mantle peridotites and slab-derived adakitic melts beneath the Japan Sea.

(2) The involvement of adakitic melts in the mantle beneath the Japan Sea consistently accounts for the geochemical characteristics of the enriched basaltic magmas formed during the opening of the Japan Sea, and the secondary orthopyroxenes in the peridotite from the Shiribeshi Seamount provide direct evidence for the metasomatic influx of slab-derived melts into the mantle beneath the Japan Sea. Adakitic metasomatism, as documented in the Japan Sea, also potentially plays an important role in mantle evolution and magma generation beneath global back-arc basins.

Acknowledgements

We thank JAMSTEC for providing the peridotite xenoliths from the archive rock samples. Robert Kay and Pat Castillo are thanked for their constructive comments.

References

Allan, J. F. and Gorton, M. P. (1992) Geochemistry of igneous rocks from Legs 127 and

128, Sea of Japan. In: Tamaki, K., Suyehiro, K., Allan, J., McWilliams, M., et al. (Eds.), Proceedings of the Ocean Drilling Program Scientific Result, 127/128, College Station, Texas (Ocean Drilling Program), 905–929.

Arai, S. and Kida, M. (2000) Origin of fine-grained peridotite xenoliths from Iraya volcano of Batan Island, Philippines: deserpentinization or metasomatism at the wedge mantle beneath an incipient arc? Island Arc 9, 458–471.

Arai, S. and Ishimaru, S. (2008) Insights into petrological characteristics of the lithosphere of mantle wedge beneath arcs through peridotite xenoliths: a review. Journal of Petrology, 49, 665–695.

Bali, E., Falus, G., Szabó, C., Peate, D. W., Hidas, K., Török, K., and Ntaflos, T. (2007) Remnants of boninitic melts in the upper mantle beneath the central Pannonian Basin? Mineralogy and Petrology, 90, 51–72.

Bali, E., Zajacz, Z., Kivács, I., Szabó, C. S., Halter, W., Vaselli, O., Török, K., and Bodnar, R. (2007) A quartz-bearing orthopyroxene-rich websterite xenolith from the Pannonian Basin, western Hungary: evidence for release of quartz-saturated melts from a subducted slab. Journal of Petrology, 49, 421–439.

Bénard, A. and Ionov, D. A. (2012) A new petrogenetic model for low-Ca boninites: Evidence from veined sub-arc xenoliths on melt-mantle interaction and melt fractionation. Geochemistry, Geophysics, Geosystems 13, Q0AF05, doi:10.1029/2012GC004145.

Bénard, A. and Ionov, D. A. (2013) Melt- and fluid-rock interaction in supra-subduction lithospheric mantle: evidence from andesite-hosted veined peridotite xenoliths. Journal of Petrology, 54, 2339–2378.

Cousens, B. L., Allan, J. F., and Gorton, M. P. (1994) Subduction-modified pelagic sediments as the enriched component in back-arc basalts from the Japan Sea: Ocean Drilling Program Sites 797 and 794. Contributions to Mineralogy and Petrology, 117, 421–434.

Drummond, M. S., Defant, M. J., and Kepezhinskas, P. K. (1996) The petrogenesis of slab derived trondhjemite–tonalite–dacite adakite magmas. Transactions of the Royal Society of Edinburgh: Earth Sciences, 87, 205—216.

Franz, L., Becker, K.-P., Kramer, W., and Herzig, P. M. (2002) Metasomatic mantle xenoliths from the Bismarck microplate (Papua New Guinea)—Thermal evolution, geochemistry and extent of slab-induced metasomatism. Journal of Petrology 43, 315–343.

Grégoire, M., McInnes, B. I.A., and O'Reilly, S. Y. (2001) Hydrous metasomatism of oceanic sub-arc mantle, Lihir, Papua New Guinea Part 2. Trace element

characteristics of slab-derived fluids. Lithos, 59, 91–108.

Halama, R., Savov, I. P., Rudnick, R. L., and McDonough, W. F. (2009) Insights into Li and Li isotope cycling and sub-arc metasomatism from veined mantle xenoliths, Kamchatka. Contributions to Mineralogy and Petrology, 158, 197–222.

Hirahara, Y., Kimura, J. –I., Senda, R., Miyazaki, T., Kawabata, H., Takahashi, T., Chang, Q., Vaglarov, B. S., Sato, T., and Kodaira, S. (2015) Geochemical variations in Japan Sea back-arc basin basalts formed by high-temperature adiabatic melting of mantle metasomatized by sediment subduction components. Geochemistry, Geophysics, Geosystems, 16, 1324–1347.

Ichiyama, Y., Soma, S., and Hanafusa, Y. (2011) The "GANSEKI" database of ocean-floor rock samples. The Journal of Geological Society of Japan, 117, 579–584 (in Japanese with English abstract).

Ichiyama, Y., Morishita, T., Tamura, A., and Arai, S. (2013) Petrology of peridotite xenolith-bearing basaltic to andesitic lavas from the Shiribeshi Seamount, off northwestern Hokkaido, the Sea of Japan. Journal of Asian Earth Sciences 76, 48–58

Ichiyama, Y., Morishita, T., Tamura, A., and Arai, S. (2016) Peridotite xenoliths from the Shiribeshi Seamount, Japan Sea: insight into mantle processes in a back-arc basin. Contributions to Mineralogy and Petrology (in submission).

Ishimaru, S., Arai, S., Ishida, Y., Shirasaka, M., and Okrugin, V. M. (2007). Melting and multi-stage metasomatism in the mantle wedge beneath a frontal arc inferred from highly depleted peridotite xenoliths from the Avacha volcano, southern Kamchatka. Journal of Petrology 48, 395–433.

Kaneoka, I., Takigami, Y., Takaoka, N., Yamashita, S., and Tamaki, K. (1992) ^{40}Ar-^{39}Ar analysis of volcanic rocks recovered from the Japan Sea floor: constraints on the age of formation of the Japan. In: Tamaki, K., Suyehiro, K., Allan, J., McWilliams, S., et al. (Eds.), Proceedings of the Ocean Drilling Program Scientific Result, 127/128, College Station, Texas (Ocean Drilling Program), 819–836.

Kelemen, P. B., Hart, S., and Berstein, S. (1998) Silica enrichment in the continental upper mantle via melt/rock reaction. Earth and Planetary Science Letters, 164, 387–406.

Kobayashi, K. and Nakamura, E. (2001) Geochemical evolution of Akagi Volcano, NE Japan: implications for interaction between island-arc magma and lower crust, and generation of isotopically various magmas. Journal of Petrology, 42, 2303–2331.

Kushiro, I. (1972) Effect of H_2O on the composition of magmas formed at high pressure. Journal of Petrology, 13, 311–334.

Li, Y.-B., Kimura, J.-I., Machida, S., Ishii, T., Ishiwatari, A., Maruyama, S., Qiu, H.-M.,

Ishikawa, T., Kato, Y., Haraguchi, S. Takahata, N., Hirahara, Y., and Miyazaki, T. (2013) High-Mg adakite and low-Ca boninite from a Bonin fore-arc seamount: Implications for the reaction between slab melts and depleted mantle. Journal of Petrology, 54, 1149–1175.

Martin, H., Smithies, R. H., Rapp, R., Moyen, J. -F., and Champion, D. (2005) An overview of adakite, tonalite–trondhjemite–granodiorite (TTG), and sanukitoid: relationships and some implications for crustal evolution. Lithos, 79, 1–24.

McDade, P., Blundy, J. D., and Wood, B. J. (2003) Trace element partitioning between mantle wedge peridotite and hydrous MgO-rich melt. American Mineralogist, 88, 1825–1831.

McDonough, W. F. and Sun, S. S. (1995) The composition of the Earth. Chemical Geology 120, 223–253.

McInnes, B. I. A., Grégoire, M., Binns, R. A., Herzig, P. M., and Hannington, M. D. (2001). Hydrous metasomatism of oceanic sub-arc mantle, Lihir, Papua New Guinea: petrology and geochemistry of fluid-metasomatised mantle wedge xenoliths. Earth and Planetary Science Letters 188, 169–183.

Morishita, T., Ishida, Y., and Arai, S. (2005) Simultaneous determination of multiple trace element compositions in thin (<30μm) layers of BCR-2G by 193 nm ArF excimer laser ablation-ICP-MS: implications for matrix effect and elemental fractionation on quantitative analysis. Geochemical Journal, 39, 327–340.

Nohda, S. (2009) Formation of the Japan Sea basin: Reassessment from Ar–Ar ages and Nd–Sr isotopic data of basement basalts of the Japan Sea and adjacent regions. Journal Asian Earth Sciences, 34, 599–609.

Otofuji, Y., Matsuda, T., and Nohda, S. (1985) Opening mode of the Japan Sea inferred from the palaeomagnetism of the Japan Arc. Nature, 317, 603–604.

Pearce, J. A. and Stern, R. J. (2006) Origin of back-arc basin magmas: trace element and isotope perspectives. In: Back-arc spreading systems: geological, biological, chemical, and physical interactions (editors: Christie, D. M., Fisher, C. R., Lee, S. -M. and Givens, S.), Geophysical Monograph Series, 166, 63–86.

Sato, M., Shuto, K., Uematsu, M., Takahashi, T., Ayabe, M., Takanashi, K., Ishimoto, H., and Kawabata, H. (2012) Origin of Late Oligocene to Middle Miocene adakites, high magnesian andesites and basalts from back-arc margin of the SW and NE Japan arcs. Journal of Petrology, 54, 481–524.

Schiano, P., Clocchiatti, R., Shimizu, N., Maury, R. C., Jochum, K. P., and Hofmann, A. W. (1995) Hydrous, silica-rich melts in the sub-arc mantle and their relationship with erupted arc lavas. Nature, 377, 595–600.

Shimizu, Y., Arai, S., Morishita, T., Yurimoto, H., and Gervilla, F. (2004) Petrochemical characteristics of felsic veins in mantle xenoliths from Tallante (SE Spain): an insight into activity of silicic melt within the mantle wedge. Transactions of the Royal Society of Edinburgh: Earth Sciences, 95, 265–276.

Shuto, K., Tsuchiya, N., Tamura, S., and Kagami, H. (1991) Geochemistry of newly discovered quaternary Shiribeshi Volcano, Northeast Japan Sea. Mineralogy and Petrology, 44, 213–234.

Takahashi, E., Uto, K., and Schilling, J.G. (1987) Primary magma compositions and Mg/Fe ratios of their mantle residues along Mid Atlantic Ridge 29ºN to 73ºN. Institute for Study of the Earth's Interior, Okayama University, Technical Report, Series A, 9, 1–14.

Tamaki, K., Suyehiro, K., Allan, J., Ingle, J. C., Jr., and Pisciotto, K. A. (1992) Tectonic synthesis and implications of Japan Sea ODP drilling. In: Tamaki, K., Suyehiro, K., Allan, J., McWilliams, M., et al. (Eds.), Proceedings of the Ocean Drilling Program Scientific Result, 127/128, College Station, Texas (Ocean Drilling Program), 1333–1348.

Tamura, Y. (2003) Genetic relationship between Quaternary NE Japan Arc magmas and Miocene Japan Sea back-arc basin basalts: implications for a dynamic model of hot fingers in the Mantle Wedge. Journal of Geology, 112, 781–793 (in Japanese with English abstract).

Tatsumi, Y. and Eggins, S. M. (1995) Subduction Zone Magmatism. Wiley, Cambridge, 211 pp.

Taylor, B. and Martinez, F. (2002) Back-arc basin basalt systematics. Earth and Planetary Science Letters, 210, 481–497.

Figure Captions

Fig. 1

Distribution of the basement geology in the northern Japan Sea (Tamaki et al., 1992) and location of the Shiribeshi Seamount. Drill sites during ODP (black dots) are also shown.

Fig. 2

The microphotographs were taken with cross-polarized light.

Fig. 3

Plots of (a) CaO and (b) Cr_2O_3 contents against Al_2O_3 content for the secondary orthopyroxenes in the Shiribeshi peridotite xenoliths. The primary orthopyroxenes in the two-pyroxene peridotites and orthopyroxene phenocrysts in the host lavas are from Ichiyama et al. (2016) and Ichiyama et al. (2012), respectively. The regression lines for the two-pyroxene peridotites are illustrated as thick gray lines. The secondary orthopyroxenes from the Avacha and Tallante peridotites are from Ishimaru et al. (2007) and Shimizu et al. (2004), respectively.

Fig. 4

Primitive mantle-normalized trace element patterns of (a) the secondary orthopyroxenes and (b) the melts in equilibrium with the secondary orthopyroxenes. For comparison, trace-element patterns of primary orthopyroxenes in the Shiribeshi two-pyroxene peridotites, a secondary orthopyroxene in an Avacha peridotite (Ishimaru et al., 2007) and an orthopyroxene phenocryst in a magnesian adakite from the IBM arc (Li et al., 2013) and in a calc-alkali andesite from the Northeast Japan arc (Akagi Volcano; Kobayashi and Nakamura, 2001) are illustrated in (a). Also, whole rock trace element patterns of the Shiribeshi basaltic to andesitic host lavas, a boninite, and an adakite from the IBM arc (Li et al., 2013), an average adakite from the Japan Sea area (from Iwaine Formation) (Sato et al. 2012), and an average adakite (Drummond et al., 1996) are illustrated in (b). McDounogh and Sun (1995) was used for normalization values.

Fig. 5

Plots of olivine Fo (= 100 × Mg / [Mg + Fe]) versus NiO contents of the two-pyroxene peridotites. The olivine compositions in equilibrium with the primary D- and E-type basalts are based on the calculation of Tamura (2003). The mantle olivine array is from Takahashi et al. (1987).

Fig. 6

Schematic illustration of adakite metasomatism in the Japan Sea. Please see the text for details.

This is a preprint, the final version is subject to change, of the American Mineralogist (MSA)
Cite as Authors (Year) Title. American Mineralogist, in press.
(DOI will not work until issue is live.) DOI: http://dx.doi.org/10.2138/am-2017-5720

Figure 1

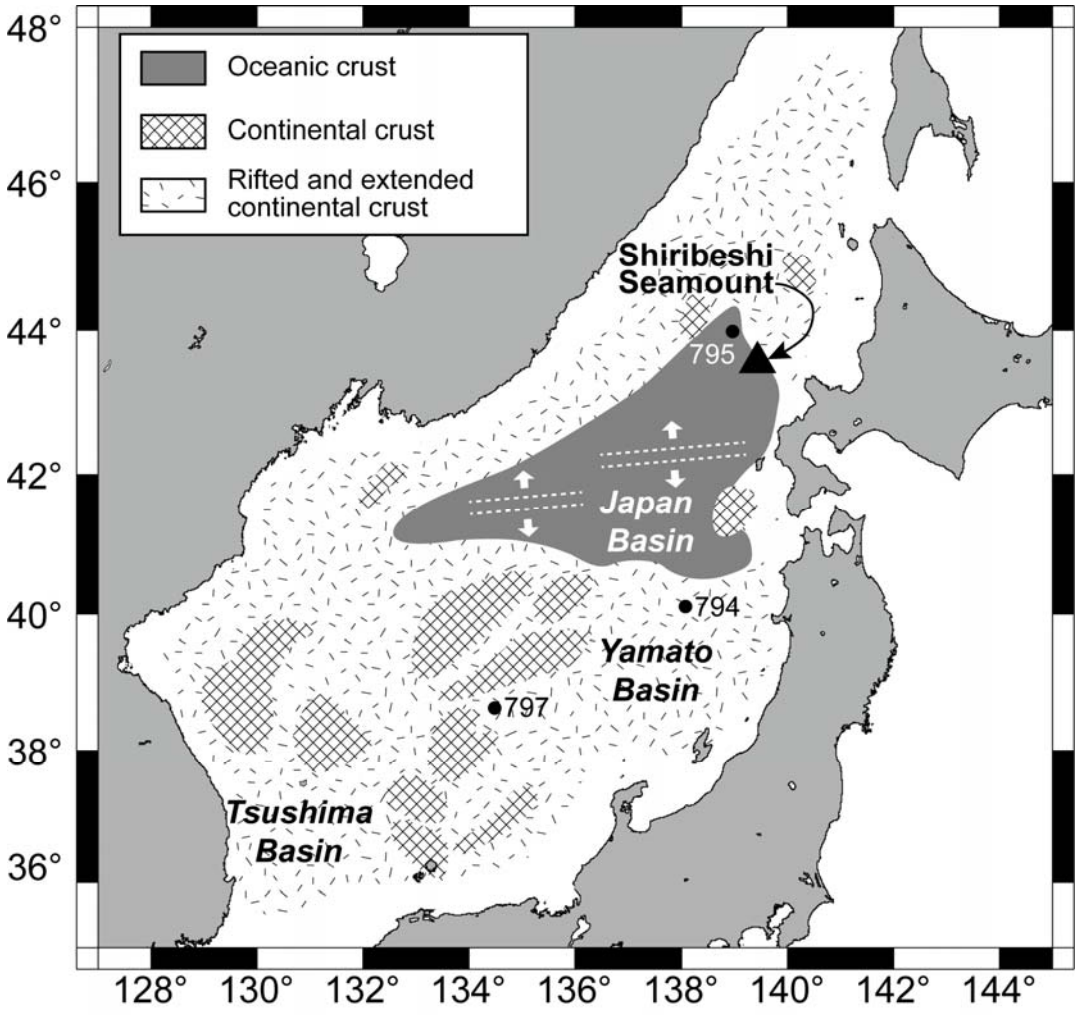

This is a preprint, the final version is subject to change, of the American Mineralogist (MSA)
Cite as Authors (Year) Title. American Mineralogist, in press.
(DOI will not work until issue is live.) DOI: http://dx.doi.org/10.2138/am-2017-5720

Figure 2

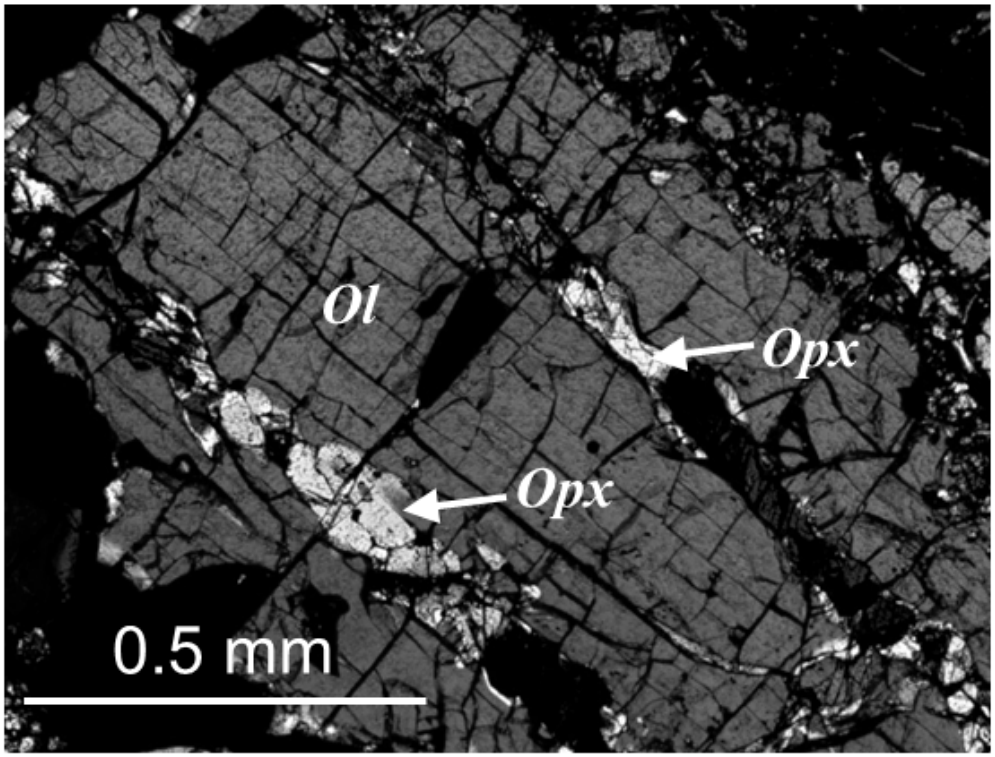

This is a preprint, the final version is subject to change, of the American Mineralogist (MSA)
Cite as Authors (Year) Title. American Mineralogist, in press.
(DOI will not work until issue is live.) DOI: http://dx.doi.org/10.2138/am-2017-5720

Figure 3

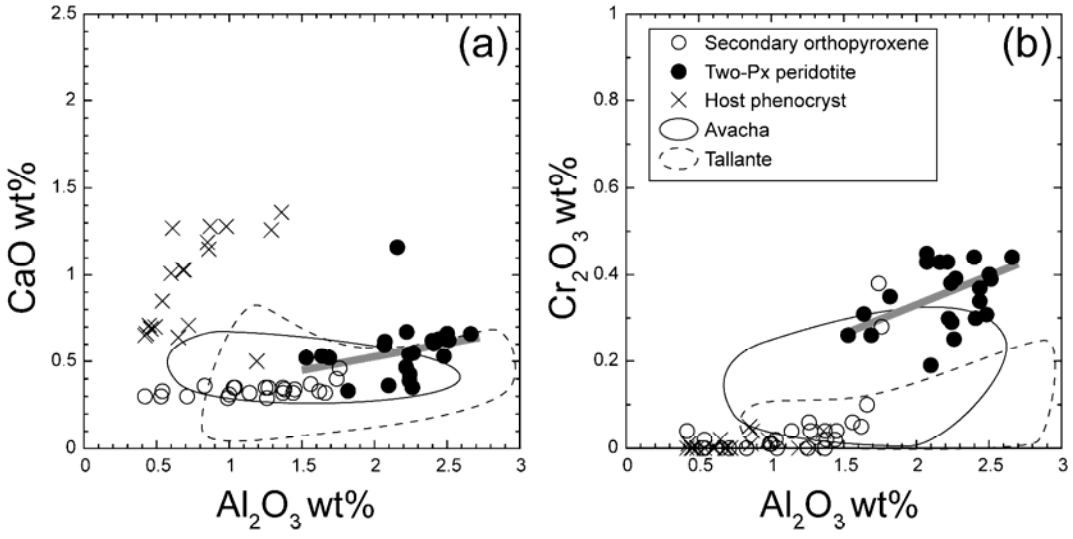

This is a preprint, the final version is subject to change, of the American Mineralogist (MSA)
Cite as Authors (Year) Title. American Mineralogist, in press.
(DOI will not work until issue is live.) DOI: http://dx.doi.org/10.2138/am-2017-5720

Figure 4

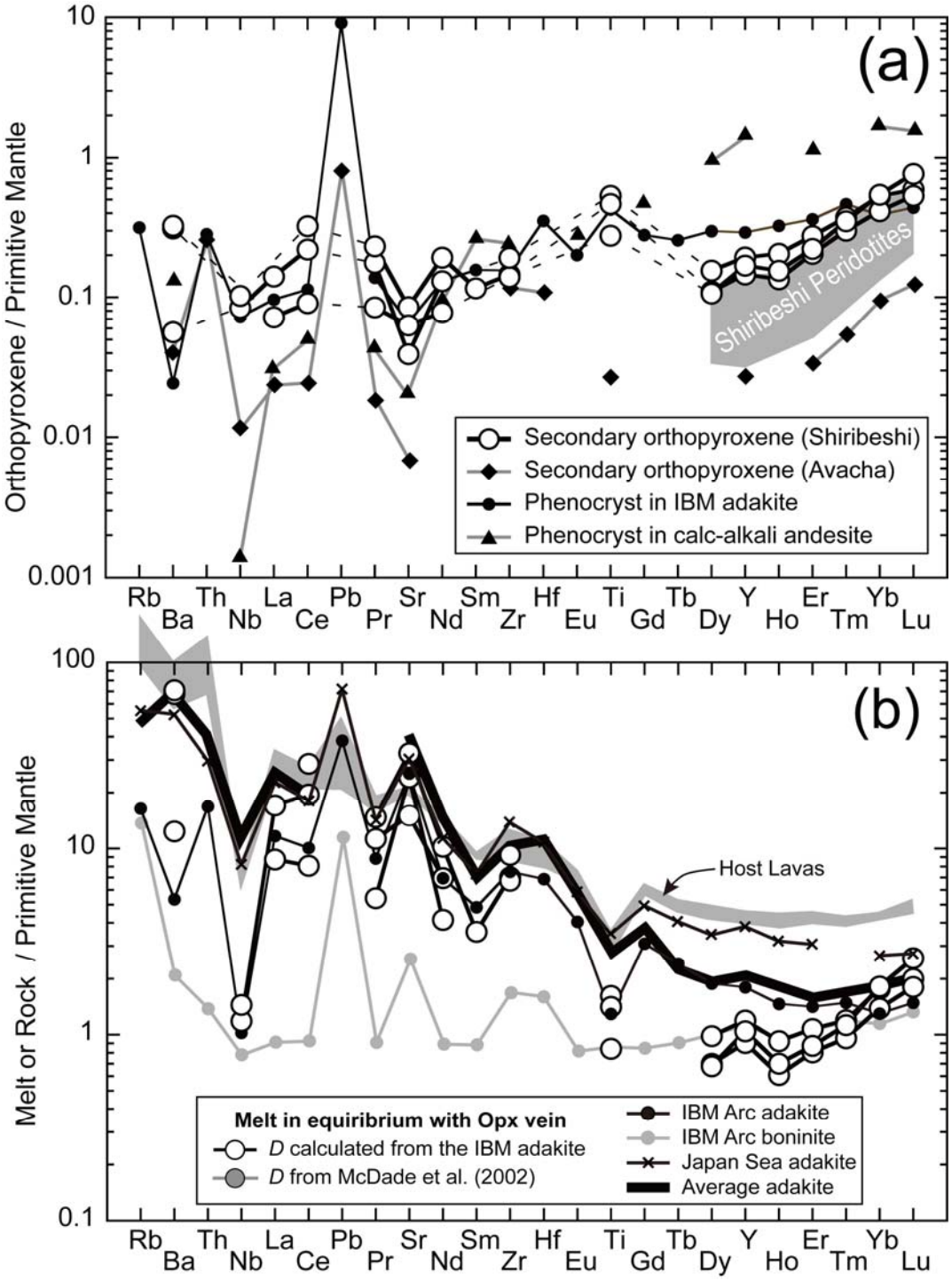

This is a preprint, the final version is subject to change, of the American Mineralogist (MSA)
Cite as Authors (Year) Title. American Mineralogist, in press.
(DOI will not work until issue is live.) DOI: http://dx.doi.org/10.2138/am-2017-5720

Figure 5

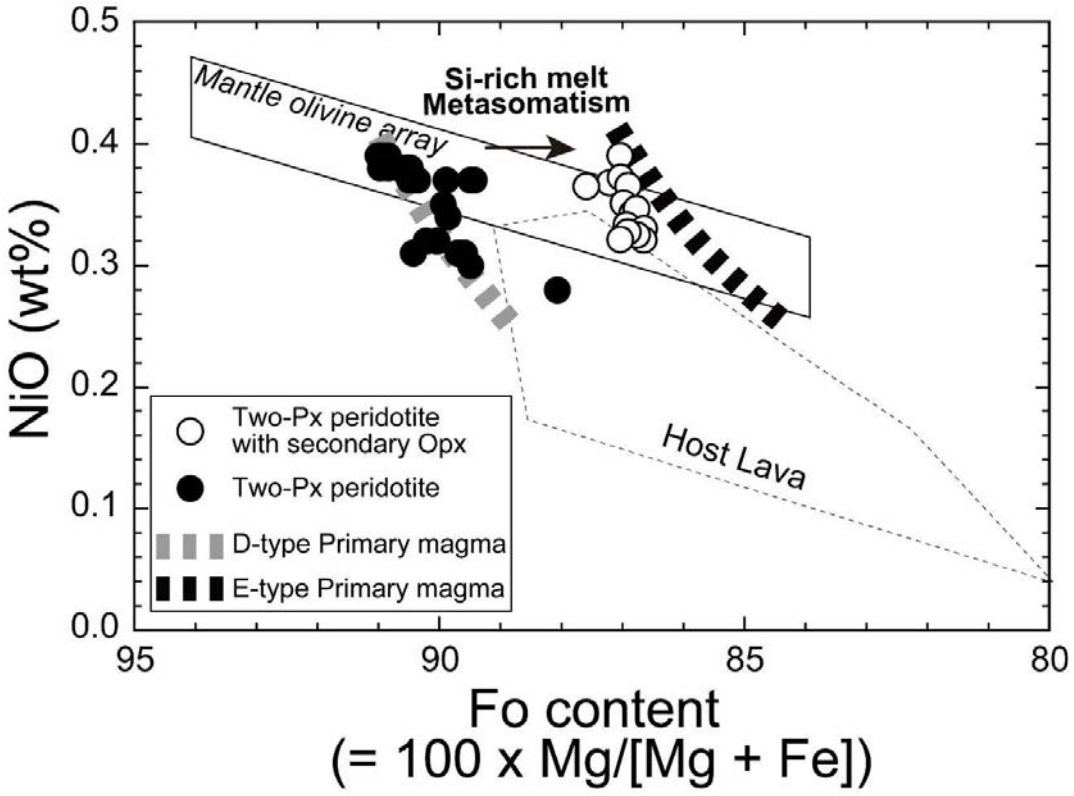

This is a preprint, the final version is subject to change, of the American Mineralogist (MSA)
Cite as Authors (Year) Title. American Mineralogist, in press.
(DOI will not work until issue is live.) DOI: http://dx.doi.org/10.2138/am-2017-5720

Figure 6

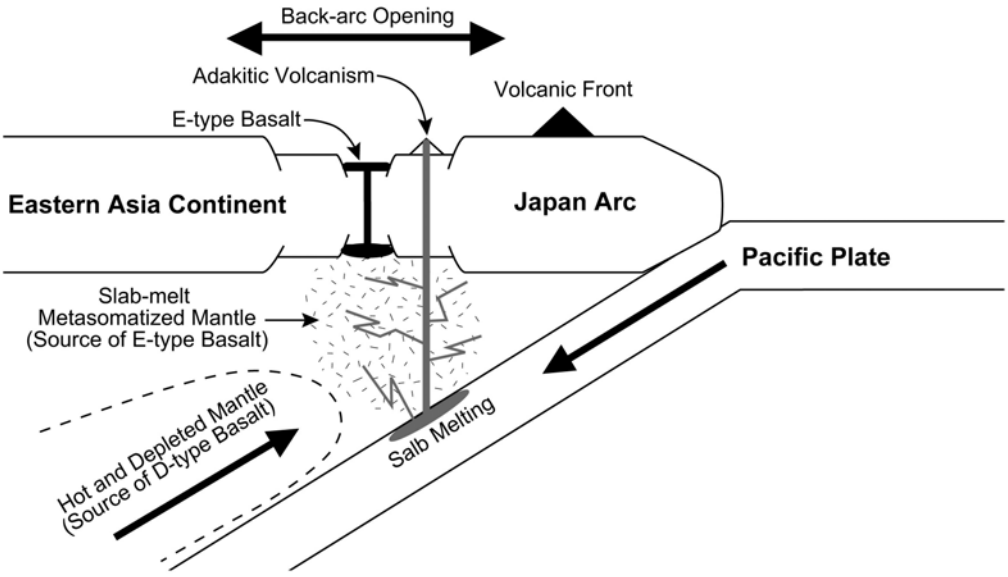

This is a preprint, the final version is subject to change, of the American Mineralogist (MSA)
Cite as Authors (Year) Title. American Mineralogist, in press.
(DOI will not work until issue is live.) DOI: http://dx.doi.org/10.2138/am-2017-5720

Table 1 Representative chemical composition of orthopyroxenes in the peridotite xenoliths from the Shiribeshi Seamount

	Secondary Orthopyroxene				Primary	
SiO_2	57.04	57.15	56.76	56.78	56.29	56.35
TiO_2	0.02	0.00	0.04	0.00	0.08	0.02
Al_2O_3	1.04	0.83	1.45	1.26	2.41	2.24
Cr_2O_3	0.00	0.00	0.04	0.06	0.30	0.29
FeO*	7.81	8.18	8.18	7.89	6.23	6.31
MnO	0.34	0.32	0.30	0.30	0.18	0.16
MgO	33.64	33.74	33.83	33.71	33.99	34.61
CaO	0.35	0.36	0.34	0.29	0.60	0.43
Na_2O	0.00	0.00	0.01	0.02	0.03	0.00
K2O	0.01	0.00	0.01	0.00	0.01	0.01
Total	100.24	100.58	100.95	100.32	100.13	100.42
O	6	6	6	6	6	6
Si	1.974	1.975	1.956	1.965	1.941	1.937
Ti	0.001	0.000	0.001	0.000	0.002	0.001
Al	0.042	0.034	0.059	0.051	0.098	0.091
Cr	0.000	0.000	0.001	0.002	0.008	0.008
Fe*	0.226	0.236	0.236	0.228	0.180	0.181
Mn	0.010	0.009	0.009	0.009	0.005	0.005
Mg	1.736	1.738	1.737	1.739	1.747	1.774
Ca	0.013	0.013	0.012	0.011	0.022	0.016
Na	0.000	0.000	0.001	0.001	0.002	0.000
K	0.000	0.000	0.000	0.000	0.001	0.000
Total	4.002	4.006	4.012	4.006	4.005	4.013
Mg#	0.885	0.880	0.881	0.884	0.907	0.907

*Total Fe as Fe^{2+}

This is a preprint, the final version is subject to change, of the American Mineralogist (MSA)
Cite as Authors (Year) Title. American Mineralogist, in press.
(DOI will not work until issue is live.) DOI: http://dx.doi.org/10.2138/am-2017-5720

Table 2 Trace element and rare earth element contentrations (ppm) of sedondary orthopyroxenes in peridotite xenoliths from the Shiribeshi Seamount and partition coefficients used for the estimation of the melt compositions.

	Orthopyroxenes			Partition coefficients	
Spot No.	#701	#702	#703	D^{*}	D^{**}
Ti	676	591	351	0.141	0.321
Rb	-	-	-	-	0.019
Sr	0.813	1.76	1.30	0.0044	0.003
Y	0.860	0.651	0.751	0.101	0.158
Zr	2.10	1.60	1.53	0.027	0.020
Nb	0.059	0.072	-	0.0028	0.070
Ba	0.387	2.12	2.22	-	0.004
La	0.095	-	0.049	0.003	0.008
Ce	0.382	0.560	0.158	0.005	0.011
Pr	0.048	0.063	0.023	-	0.015
Nd	0.173	0.254	0.103	0.009	0.018
Sm	-	0.050	-	0.021	0.032
Eu	-	-	-	0.031	0.049
Gd	-	-	-	-	0.088
Tb	-	-	-	-	0.104
Dy	0.112	0.080	0.077	-	0.155
Ho	0.033	0.022	0.025	-	0.217
Er	0.129	0.096	0.105	0.121	0.250
Tm	0.027	0.022	0.025	-	0.305
Yb	0.253	0.199	0.261	0.164	0.291
Lu	0.043	0.038	0.055	0.186	0.288

*: McDate et al. (2003)

**: Calculated from orthopyroxene / host rock of the IBM adakite (sample: D22-53) from Li et al. (2013)